

Group velocity inversion in AlGaAs nanowires

J. Meier, W. S. Mohammed, A. Jugessur, L. Qian, M. Mojahedi and J. S. Aitchison

*Department of Electrical and Computer Engineering,
University of Toronto, Toronto, Ontario, Canada, M5S 3G4*

Abstract: We investigated the dispersion characteristics of submicron sized AlGaAs waveguides. Numerical simulations shows that the tight confinement of the optical waves in such nanowires leads to strong variations of the dispersion characteristics compared to classic, weakly guided waveguides of the same material system. We found numerically that the investigated structure has negative GVD for the TE mode provided the waveguide width is between 670 nm and 280 nm. Experimental data obtained from 300 μm - 1 mm long wires confirms the numerical results.

©2007 Optical Society of America

OCIS codes: (230.3120) Integrated optics devices, (230.7380) Waveguides, channels

References and links

1. P. N. Prasad, *Nanophotonics* (John Wiley and Sons, New York, 2004).
2. M. A. Foster, J. M. Dudley, B. Kibler, Q. Cao, D. Lee, R. Trebino, and A. L. Gaeta, "Nonlinear pulse propagation and supercontinuum generation in photonic nanowires: experiment and simulation," *Appl. Phys. B* **81**, 363-367 (2005).
3. S. G. Leon-Saval, T. A. Birks, W. J. Wadsworth, P. S. J. Russell, and M. W. Mason, "Supercontinuum generation in submicron fibre waveguides," *Opt. Express* **12**, 2864-2869 (2004).
4. Y. K. Lize, E. C. Magi, V. G. Ta'eed, J. A. Bolger, P. Steinvurzel, and B. J. Eggleton, "Microstructured optical fiber photonic wires with subwavelength core diameter," *Opt. Express* **12**, 3209-3217 (2004).
5. V. R. Almeida, C. A. Barrios, R. R. Panepucci, and M. Lipson, "All-optical control of light on a silicon chip," *Nature* **431**, 1081-1084 (2004).
6. A. C. Turner, C. Manolatu, B. S. Schmidt, M. Lipson, M. A. Foster, J. E. Sharping, and A. L. Gaeta, "Tailored anomalous group-velocity dispersion in silicon channel waveguides," *Opt. Express* **14**, 4357-4362 (2006).
7. M. A. Foster, A. C. Turner, J. E. Sharping, B. S. Schmidt, M. Lipson, and A. L. Gaeta, "Broad-band optical parametric gain on a silicon photonic chip," *Nature* **441**, 960-963 (2006).
8. S. F. Preble, Q. Xu, B. S. Schmidt, and M. Lipson, "Ultrafast all-optical modulation on a silicon chip," *Opt. Lett.* **30**, 2891-2893 (2005).
9. B. G. Lee, B. A. Small, K. Bergman, Q. Xu and M. Lipson, "Transmission of high-data-rate optical signals through a micrometer-scale silicon ring resonator," *Opt. Lett.* **31**, 2701-2703 (2006).
10. G. I. Stegeman, A. Villeneuve, J. Kang, J. S. Aitchison, C. N. Ironside, K. Alhemyari, C. C. Yang, C. H. Lin, H. H. Lin, G. T. Kennedy, R. S. Grant, and W. Sibbett, "Algaas Below Half Bandgap - the Silicon of Nonlinear-Optical Materials," *Int. J. Nonlinear Opt. Phys.* **3**, 347-371 (1994).
11. J. S. Aitchison, A. H. Kean, C. N. Ironside, A. Villeneuve, and G. I. Stegeman, "Ultrafast All-Optical Switching in Al_{0.18}Ga_{0.82}As Directional Coupler in 1.55 μm Spectral Region," *Electron Lett.* **27**, 1709-1710 (1991).
12. J. S. Aitchison, K. Alhemyari, C. N. Ironside, R. S. Grant, and W. Sibbett, "Observation of Spatial Solitons in Algaas Wave-Guides," *Electron Lett.* **28**, 1879-1880 (1992).
13. J. U. Kang, G. I. Stegeman, and J. S. Aitchison, "One-dimensional spatial soliton dragging, trapping, and all-optical switching in AlGaAs waveguides," *Opt. Lett.* **21**, 189-191 (1996).
14. H. S. Eisenberg, Y. Silberberg, R. Morandotti, A. R. Boyd, and J. S. Aitchison, "Discrete spatial optical solitons in waveguide arrays," *Phys. Rev. Lett.* **81**, 3383-3386 (1998).
15. G. A. Siviloglou, S. Sunsov, R. El-Ganainy, R. Iwanow, G. I. Stegeman, D. N. Christodoulides, R. Morandotti, D. Modotto, A. Locatelli, C. De Angelis, F. Pozzi, C. R. Stanley, and M. Sorel, "Enhanced third-order nonlinear effects in optical AlGaAs nanowires," *Opt. Express* **14**, 9377-9384 (2006).
16. R. El-Ganainy, S. Mokhov, K. G. Makris, D. N. Christodoulides, and R. Morandotti, "Solitons in dispersion-inverted AlGaAs nanowires," *Opt. Express* **14**, 2277-2282 (2006).
17. S. Gehrsitz, F. K. Reinhart, C. Gourgon, N. Herres, A. Vonlanthen, and H. Sigg, "The refractive index of Al_xGa_{1-x}As below the band gap: Accurate determination and empirical modeling," *J. Appl. Phys.* **87**, 7825-7837 (2000).

1. Introduction

Recent interest in high contrast waveguides has developed into an intense topic of research [1-4]. This was primarily driven by the availability of advanced processing technology, especially regarding Silicon-on-Insulator (SOI) structures. SOI nanoscale waveguides have been shown to provide high confinement [5], and hence strong nonlinear interactions between light and matter, as well as having the possibility to modify the temporal dispersion characteristics [6]. The combination of these effects has led to the demonstration of broadband parametric amplification in such devices [7]. However, though significant progress has been made towards all-optical silicon devices [8, 9], due to strong carrier dynamics close to the bandgap and relatively long recovery times, silicon is generally not a material of choice for ultrafast nonlinear devices.

AlGaAs has been shown to have a strong, ultrafast Kerr nonlinearity when used at wavelengths around 1.55 μm . This operation wavelength is lower than half the bandgap energy of $\text{Al}_{0.2}\text{Ga}_{0.8}\text{As}$, and hence linear and two photon absorption are negligible [10]. AlGaAs has been used to demonstrate many interesting nonlinear effects, such as self-phase modulation (SPM) [10], all optical switching in nonlinear directional couplers [11] and numerous soliton experiments [12-14]. Despite the strong Kerr nonlinearity of AlGaAs, practical applications have been limited by the power requirements of the weakly guiding structures.

In contrast, high index contrast AlGaAs waveguides offer the potential to reduce the power needed for switching applications due to increased field confinement. Recently, the first observations of SPM in submicron AlGaAs nanowires have been fabricated and strong SPM has been observed [15].

Similar high field confinement SOI waveguides show drastic modifications of the dispersion characteristics [6, 7]. Recently, cylindrical AlGaAs nanowires have been theoretically investigated, and it was found that it is possible to invert the group velocity dispersion (GVD) for rods with around 400 nm diameter [16]. In this paper we present a numerical and experimental investigation of the dispersion properties for a recently implemented AlGaAs nanowire with rectangular core [15] and show that this structure exhibits strong GVD inversion for submicron wide waveguides. We present detailed information on the dispersion characteristics for varying core dimension and wavelength.

2. Waveguide structure

The structure under consideration is shown in Fig. 1. A core of height h consisting of $\text{Al}_{0.2}\text{Ga}_{0.8}\text{As}$ is embedded between a cladding and a buffer layer of $\text{Al}_{0.7}\text{Ga}_{0.3}\text{As}$. The index difference between core and the surrounding layers is on the order of 0.2, high enough to confine the mode tightly in the core layer. The 4 μm thick buffer layer separates the waveguide core from a GaAs substrate (not shown in Fig. 1).

A two dimensional confined waveguide is formed by etching a pillar of width w . We assume that the etch depth ($\sim 2.7 \mu\text{m}$) and the separation between waveguide core the substrate is large enough to make leakage into the GaAs substrate negligible and omit the substrate during our calculations. The refractive index dispersion of the different layers is based on the model presented by Gehrsitz et al. [17]. We used the commercial finite element mode-solver Comsol 3.2 for our simulations.

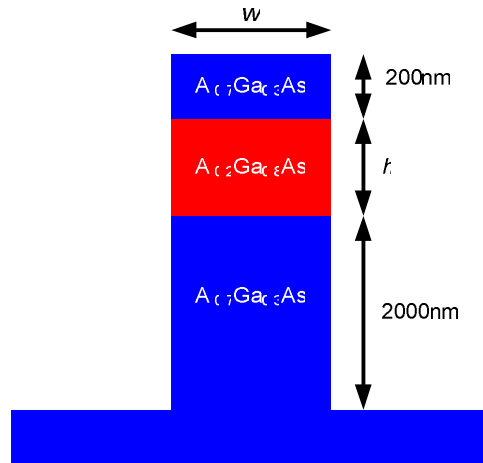


Fig. 1. Structure

3. Numerical results

We show example of the TE mode for a 250 nm wide waveguide with a 500 nm core height in Fig. 2. The strong index-step between the ridge and the surrounding layers results in confinement of most of the optical power in the core region. However, part of the mode extends into the air layer, giving rise to a decrease of the effective mode index below the index of the core and strong modification of the dispersion characteristics of such structures.

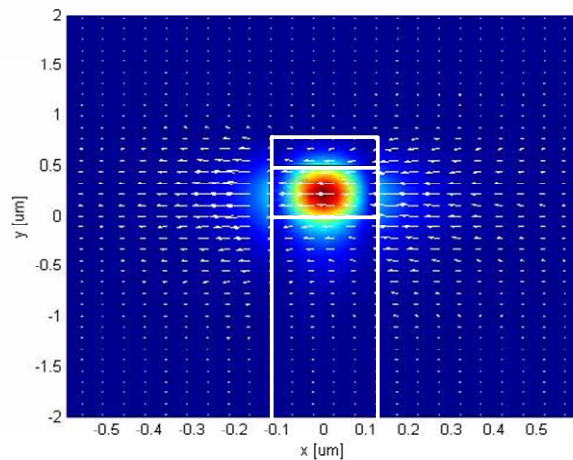


Fig. 2. Example of a TE mode for 250 nm wide waveguide. (Arrow: electric field)

We investigated the influence of the core dimension on the group velocity dispersion $\beta'' = d^2\beta/d\omega^2$ for the TE mode to determine optimum core dimensions and show the results in Fig. 3. Considering constraints such as efficient excitation of the modes and the need of a small effective index we investigated possible core heights between 0.3 and 0.8 μm . We find that for a waveguide width of less than approximately 650 nm the GVD becomes inverted. The anomalous GVD is found to exceed $-4.5 \text{ ps}^2\text{m}^{-1}$ for waveguide width of about 350 nm and core height of more than 450 nm. The region of inverted GVD is only weakly depending

on the core height and we limit our further investigation to the case of a core height of 500 nm.

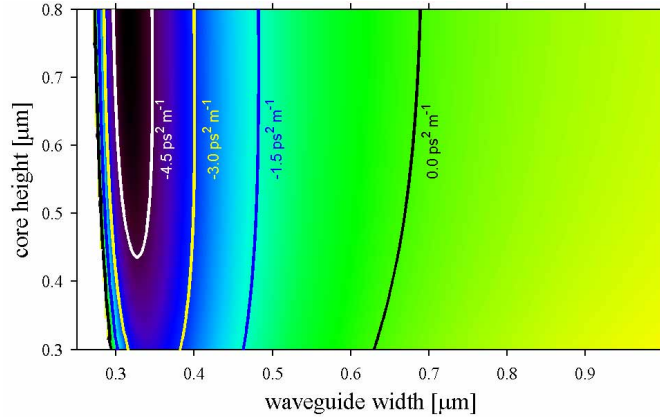


Fig. 3. GVD dependence on waveguide width and core height at a wavelength of 1.55 μm .

The TE mode GVD as a function of width and wavelength is shown in Fig. 4 for a fixed core height of 500 nm. The wavelength range is centered on 1.55 μm because this will be the optimum operation wavelength for nonlinear devices in AlGaAs.

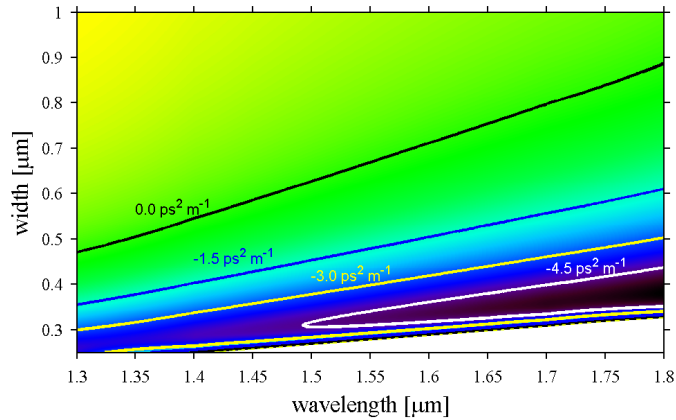


Fig. 4. GVB vs. wavelength and width. ($h = 0.5 \mu\text{m}$)

The effective index of the TE and TM modes for different waveguide widths and a constant core height of 500 nm operating at a wavelength of 1.55 μm is shown in Fig. 5. For wide waveguides the effective index is close to the refractive index of the core material. For decreasing width the effective index changes rapidly, while the mode extends more and more into the air surrounding the waveguide (see Fig. 2 for an example of a TE mode). For a waveguide width below 1.2 μm the TM_{00} mode becomes the fundamental mode. The TE mode reaches its cut-off width at 200 nm while the TM mode is still guided at less than 100 nm width. Also shown are the effective indices for the TE_{10} and TM_{10} modes. The device operates in single mode for a width less than 500 nm (300 nm) for the TE (TM) polarization.

4. Experimental results

We fabricated nanowires with lengths, d_{wire} , of 300/600/1000 μm by ebeam-lithography and reactive ion etching on a grown AlGaAs wafer with a core height of 500 nm. The wires were feed by a 2 μm wide waveguide and a $d_{\text{taper}} = 150 \mu\text{m}$ long taper as shown in Fig. 6. The full

structure was $d = 2.4$ mm long. In each nanowires set an extra sample with no wire is fabricated to calibrate for the dispersion caused by the feed and taper. An SEM image of nanowires, tapers and feed waveguides is shown in Fig. 7(a) and the different sections parameters are presented in table 1.

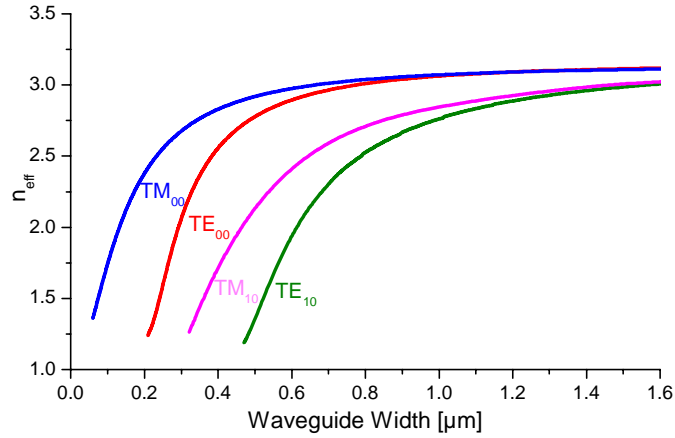


Fig. 5. Effective index of TE₀₀ and TM₀₀ vs. waveguide width for a wavelength of 1.55 μm .

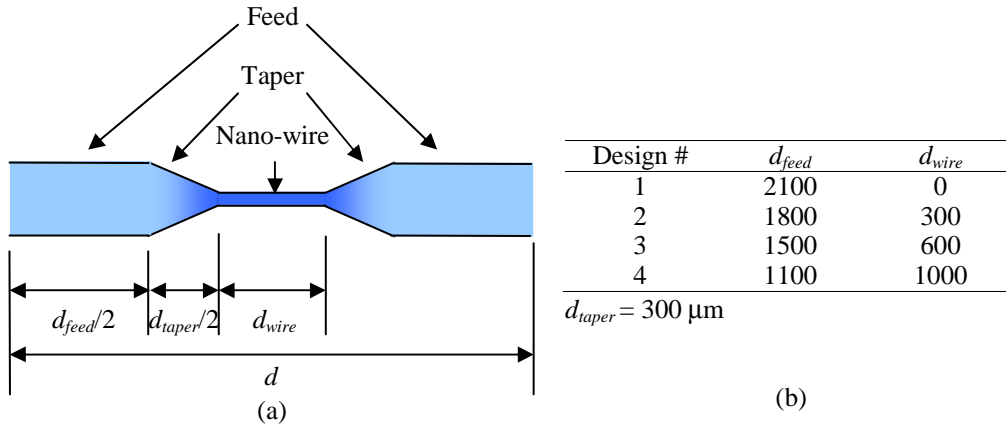


Fig. 6. (a) Nano-wire general structure with tapering and feed. (b) The length parameters for the four different designs.

To experimentally verify our predictions we measured the Fabry-Perot interference pattern using an OSA and an ASE source amplified by a EDFA. The change of the fringe period with wavelength is measured by first dividing the whole source bandwidth into smaller bands (2 nm wide spectral regions of the full measurement range between 1525 nm and 1575 nm). The average period in each band is calculated using a Fourier transform. The measured fringe periods for wires of 340 nm width is shown in Fig.7(b).

The fringe period, Λ , is directly related to the first derivative of β with respect to λ as

$$\frac{d\beta}{d\lambda} = \frac{\pi}{\Lambda d}$$

To calculate the group effective index n_g and the group velocity dispersion β'' ,

$$\frac{d^2\beta}{d\lambda^2}$$

is extracted by fitting the data with a second order polynomial

$$\Lambda = \Lambda_0 + \Lambda_1(\lambda - \lambda_0) + \frac{1}{2}\Lambda_2(\lambda - \lambda_0)^2 \quad (1)$$

and

$$\frac{d^2\beta}{d\lambda^2} = -\frac{\pi}{\Lambda_0^2 d} \Lambda_1. \quad (2)$$

n_g and β'' are then found by using:

$$n_g = -\frac{\lambda^2}{2\pi} \frac{d\beta}{d\lambda} \quad (3)$$

$$\beta'' = \frac{\lambda^3}{(2\pi c)^2} \left[2 \frac{d\beta}{d\lambda} + \lambda \frac{d^2\beta}{d\lambda^2} \right] \quad (4)$$

Having nanowires of different length allowed us to eliminate the effect of the feed waveguides and the tapers and determine group index n_g and β'' .

$$\beta''_{total} d = \beta''_{feed} d_{feed} + \beta''_{taper} d_{taper} + \beta''_{wire} d_{wire} \quad (5)$$

where $d = d_{feed} + d_{taper} + d_{wire}$.

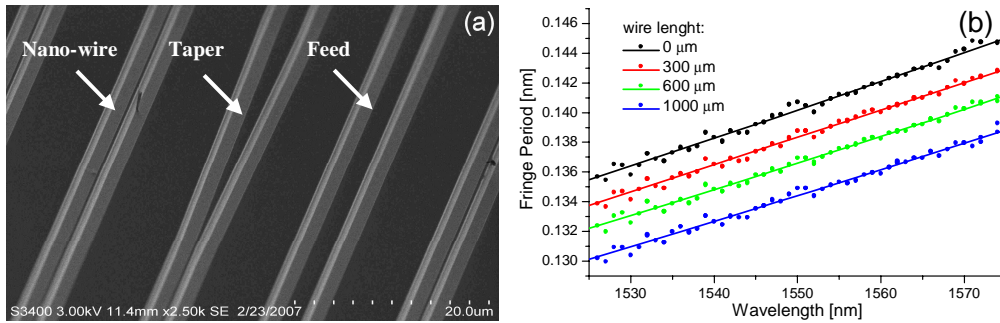


Fig. 7. (a) SEM image of fabricated nanowires. (b) Fringe period determined from measured spectra

Fig. 8 shows the group index for the TE_{00} and the TM_{00} mode. The TE mode shows a strong increase of the group index for waveguide width lower than 500 nm, while both modes show the expected convergence towards the material group index for wide waveguides. Also shown is the experimentally obtained group index. The horizontal error bar indicates a fabrication related increase of the width compared to the design width.

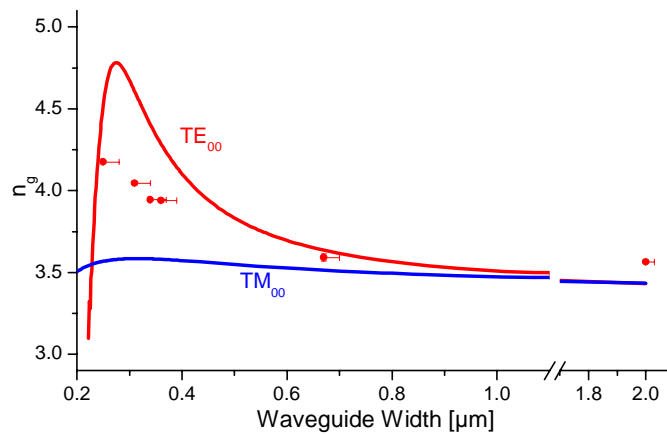


Fig. 8. Group index n_g vs. waveguide width for a wavelength of 1.55 μm .

In Fig. 9 we show β'' for a wavelength of 1.55 μm . For waveguide widths below 1 μm the strong field confinement dominates over the material dispersion and leads to an inversion of the GVD of the TE mode for waveguide widths between 670 nm and 281 nm. The maximum anomalous GVD of $-4.73 \text{ ps}^2 \text{ m}^{-1}$ is reached for a width of 323 nm. The TM mode, whose electric field is continuous across the strong index step between AlGaAs and air, shows no GVD inversion. However, for small width (less than 300 nm) the TM GVD starts to strongly increase when approaching the cutoff width.

We also show measured values of β'' . As can be seen we confirm the existence of GVD inversion for width of 350 nm. Here, the vertical errorbars have been obtained by bootstrapping the measured fringe periods and indicate the standard deviation of the data.

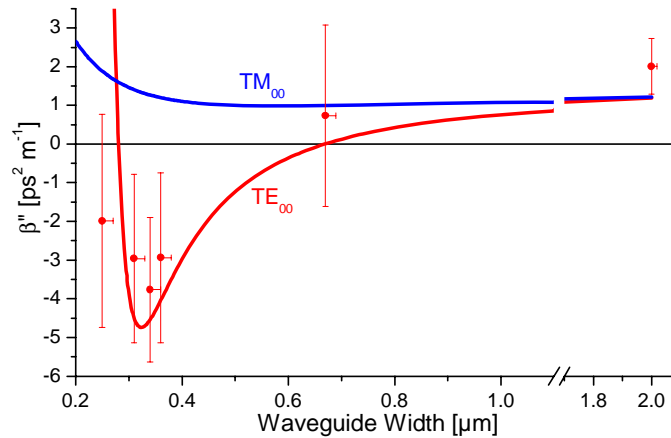


Fig. 9. GVD vs. waveguide width for a wavelength of 1.55 μm .

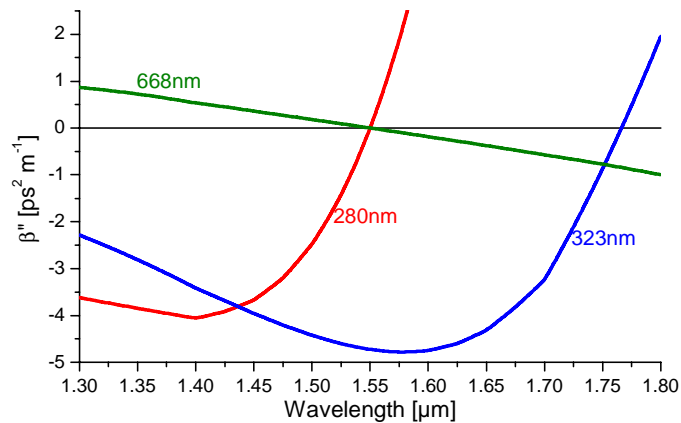


Fig. 10. GVD vs. wavelength for width of 668 nm, 323 nm and 280 nm. (core height = 0.5 μm)

In Fig. 10 we show the evolution of the GVD vs. wavelength for three different widths. The examples chosen correspond to the two widths having zero GVD around 1.55 μm (668 nm and 280nm width) and the maximal negative GVD at 323 nm width. We see that higher order dispersion terms become significant for small waveguide widths, especially if the intended design goes towards zero GVD at small width. The GVD of the 323 nm wide waveguide shows only weak dependency on wavelength near 1550 nm. The combination of

strong negative β'' with weak higher order dispersion makes this waveguide width ideal for the observation of temporal solitons.

For the use of such high contrast waveguides in nonlinear devices the effective area

$$A_{eff} = \frac{\left[\iint I(x, y) dx dy \right]^2}{\iint_{Core} I^2(x, y) dx dy} \quad (6)$$

is of high interest. We show A_{eff} for the 500 nm height core and a wavelength of 1.55 μm in Fig. 11. For the TE mode a minimum area is reached for a waveguide width of 335 nm with $A_{eff} = 0.21 \mu\text{m}^2$. This waveguide width coincides with the maximum negative GVD. It is about a factor of 50 lower than the effective area of regular AlGaAs waveguides, potential opening the possibility to demonstrate mm long nonlinear switching devices with Watt-level power requirements.

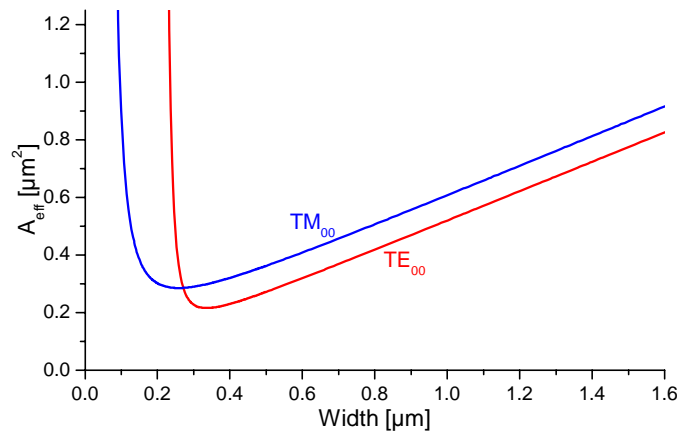


Fig. 11. Effective area vs. waveguide width for a core height of 500 nm and a wavelength of 1.55 μm

5. Conclusions

We investigated numerically and experimentally the temporal dispersion characteristics of high index contrast AlGaAs nanowires. For a proper choice of the waveguide dimensions, strong anomalous GVD is predicted and observed for the TE mode of the proposed structure. A maximal anomalous GVD of $\beta'' = -4.73 \text{ps}^2 \text{m}^{-1}$ has been calculated. We achieved good agreement between numerical predictions and experiments. The sign and magnitude of the GVD combined with the low effective area on the order of $0.21 \mu\text{m}^2$ could allow the observation of temporal solitons in mm-long AlGaAs samples or be used for efficient wavelength converters based on four wave mixing.

Acknowledgments

The authors would like to thank Dr. M. Sorel of the University of Glasgow for assisting the waveguide fabrication.